

# Microwave dielectric properties of $\text{Ba}_2\text{Ti}_9\text{O}_{20}$ materials prepared by reaction sintering process

Chi-Ben Chang<sup>a,\*</sup>, Keh-Chyang Leou<sup>a</sup>, Wen-Yang Shu<sup>b</sup>, I-Nan Lin<sup>c</sup>

<sup>a</sup> Department of System and Engineering Science, National Tsing-Hua University, Hsinchu 300, Taiwan, ROC

<sup>b</sup> Materials & Electro-Optics Research Division, Chung-Shan Institute of Science & Technology, Lung-Tan, Taiwan, ROC

<sup>c</sup> Department of Physics, Tamkang University, Tamsui 251, Taiwan, ROC

Available online 20 December 2005

## Abstract

We synthesized the  $\text{Ba}_2\text{Ti}_9\text{O}_{20}$  materials by direct reacting the nano-sized  $\text{BaTiO}_3$  with  $\text{TiO}_2$  powders. Pure Holland-like structure was obtained when the mixture of the nano-powders were calcined at  $1100^\circ\text{C}$ . The influence of the processing method on the characteristics of the  $\text{Ba}_2\text{Ti}_9\text{O}_{20}$  powders and the related microwave dielectric properties for the sintered  $\text{Ba}_2\text{Ti}_9\text{O}_{20}$  materials was investigated. The combined high-energy-milling and ball-milling (HeM/BM) process results in pronounced improvement for the sinterability of the  $\text{Ba}_2\text{Ti}_9\text{O}_{20}$  powders such that the samples attain a density higher than 96.2% T.D. when sintered at  $1200^\circ\text{C}/4\text{h}$ . Such a sintering temperature is significantly lower than the one needed for densifying the BM-processed samples to the same high density ( $1350^\circ\text{C}/4\text{h}$ ). However, the HeM/BM-processed samples show pronouncedly inferior microwave quality factor ( $Q \times f$ -value) to the BM-processed ones. Raman spectroscopic and SEM microstructural analyses imply that the prime factor resulting in lower  $Q \times f$ -value for HeM/BM-processed samples is the incomplete development of the granular structure. © 2005 Elsevier Ltd. All rights reserved.

**Keywords:** Milling; Dielectric properties;  $\text{BaTiO}_3$  and titanates; Microwave materials

## 1. Introduction

$\text{Ba}_2\text{Ti}_9\text{O}_{20}$  phase was first reported by Jonker and Kwestroo in  $\text{BaO-TiO}_2\text{-SnO}_2$  ternary system<sup>1</sup> and was observed to possess marvellous microwave dielectric properties, including high dielectric constant and large quality factor, by O'Bryan et al.<sup>2</sup> Since then the modification on microwave properties of  $\text{Ba}_2\text{Ti}_9\text{O}_{20}$  materials via the addition of dopants<sup>3–7</sup> was widely investigated. However, the reported results are quite controversial, which is mainly due to the difficult in forming single phase Hollandite-like structured  $\text{Ba}_2\text{Ti}_9\text{O}_{20}$  materials. Secondary phases, such as  $\text{BaTi}_4\text{O}_9$  or  $\text{BaTi}_5\text{O}_{11}$ , were observed to form preferentially in the calcinations of  $\text{BaO-TiO}_2$  mixture<sup>8</sup> that hinder the formation of Hollandite-like structured  $\text{Ba}_2\text{Ti}_9\text{O}_{20}$  phase. Co-precipitation process, which mixed the cations in atomic scale and synthesized the powders in obviously low temperature, can produce multiple-metallic-oxides with better homogeneity and higher activity.<sup>9–14</sup> However, the disadvantage in this process in the difficulty in stoichiometry control, as the co-precipitation process is sensitive to the pH-

value and temperature of the solution. To circumvent such kind of difficulty, we start with nano-sized  $\text{BaTiO}_3$  powders, mixing with proper amount of  $\text{TiO}_2$  and then processed by a conventional mixed oxide process. Moreover, the high energy milling (HeM) and ball-milling (BM) techniques were used for pulverization process, such that the particle size of the powders can be further decreased and the activity of the powders can be improved. It is expected that  $\text{Ba}_2\text{Ti}_9\text{O}_{20}$  powders possessing both high precision in composition and high sinterability can be obtained. The microwave dielectric properties of the sintered  $\text{Ba}_2\text{Ti}_9\text{O}_{20}$  materials can be improved.

## 2. Experimental

Nano-sized  $\text{BaTiO}_3$  powders (50 nm) were mixed with nano-sized  $\text{TiO}_2$  powders ( $\sim 100\text{ nm}$ ) in a nominal composition of  $\text{Ba}_2\text{Ti}_9\text{O}_{20}$ . The mixtures were calcined at  $950\text{--}1150^\circ\text{C}$  for 4 h in air, followed by pulverization–granulation–pelletization process and then were sintered at  $950\text{--}1150^\circ\text{C}$  for 4 h in air. Two pulverization techniques were used for disintegrating the calcined powders, i.e., conventional ball-milling (BM) and high-energy-milling (HeM) process. The morphology of the as-prepared  $\text{Ba}_2\text{Ti}_9\text{O}_{20}$  powders and microstructure of the

\* Corresponding author.

sintered  $\text{Ba}_2\text{Ti}_9\text{O}_{20}$  samples were examined using scanning electron microscopy (Jeol 6700F). The crystal structure of the calcined powders and sintered samples was examined using X-ray diffractometry (Rigaku D/max-II). The density of the sintered materials was measured using Archimedes method. The microwave dielectric constant ( $K$ ) and  $Q \times f$ -value of the  $\text{Ba}_2\text{Ti}_9\text{O}_{20}$  samples were measured using a cavity method at 7–8 GHz.

### 3. Results and discussion

The nano-sized  $\text{BaTiO}_3$  powders are so active that the Hollandite-like  $\text{Ba}_2\text{Ti}_9\text{O}_{20}$  phase can be obtained by calcining the  $\text{BaTiO}_3$ – $\text{TiO}_2$  mixture at a temperature higher than  $1050^\circ\text{C}$  (not shown). X-ray diffraction patterns shown in Fig. 1(a) reveal that all the BM-processed samples are of Hollandite-like structure, containing no secondary phases, regardless of the sintering temperature. In contrast, the XRD patterns shown in Fig. 1(b) exhibit that all of the HeM-processed samples, which were sintered at  $1200$ – $1320^\circ\text{C}$  (4 h), contain  $\text{TiO}_2$  rutile phase.

The powder preparation method, conventional ball-milling (BM) or high-energy-milling (HeM) processes, also markedly influence the densification behavior for the  $\text{Ba}_2\text{Ti}_9\text{O}_{20}$  materials. Fig. 2(a) (curve I) shows that, for the materials made of conventional BM process, the sintered density for the samples increases with the sintering temperature and it requires at least  $1350^\circ\text{C}$  (4 h) to achieve a density higher than 96.5% T.D. (theoretical density). In contrast, for the materials prepared by HeM-process, it needs only  $1200^\circ\text{C}$  (4 h) to densify the samples to a density higher than 94% T.D. (curve II, Fig. 2(a)). It is quite interesting to observe that the sintered density of the samples decreases monotonously with the sintering temperature and the samples sintered at  $1350^\circ\text{C}$  (4 h) were melted. These results indicate that the HeM-processed powders are extremely active.

The microwave dielectric properties for these materials also change significantly with the powder preparation process. Fig. 2(b) reveals that the  $K$ -value of the BM-processed samples increases with the sintering temperature and is largest for the samples sintered at  $1325^\circ\text{C}$  (4 h) (curve I), whereas those of the HeM-processed samples is largest for  $1200^\circ\text{C}$  (4 h)-sintered samples and decreases monotonously with sintering temperature (curve II, Fig. 2(b)). The dielectric constant ( $K$ ) of samples correlates with their sintered density intimately. The quality factor for these materials shows even more marked dependence on the powder preparation process. Fig. 2(c) indicates that the  $Q \times f$ -value of the BM-processed samples is largest for the one sintered at  $1325$ – $1350^\circ\text{C}$  (4 h) ( $Q \times f = 26,000$ , curve I), whereas those of the HeM-processed samples increases monotonously with sintering temperature, showing largest value for  $1325^\circ\text{C}$  (4 h)-sintered ones ( $Q \times f = 10,000$ , curve II).

It is quite unexpected to observe that the  $Q \times f$ -value of HeM-processed samples is so much lower than those for BM-processed ones. To understand the mechanism resulting in inferior  $Q \times f$ -value for the HeM-processed samples, the microstructural characteristics of these materials were investigated. Typical SEM micrographs shown in Fig. 3(a) and (b) indicate that the microstructure of the HeM-processed materials is signifi-

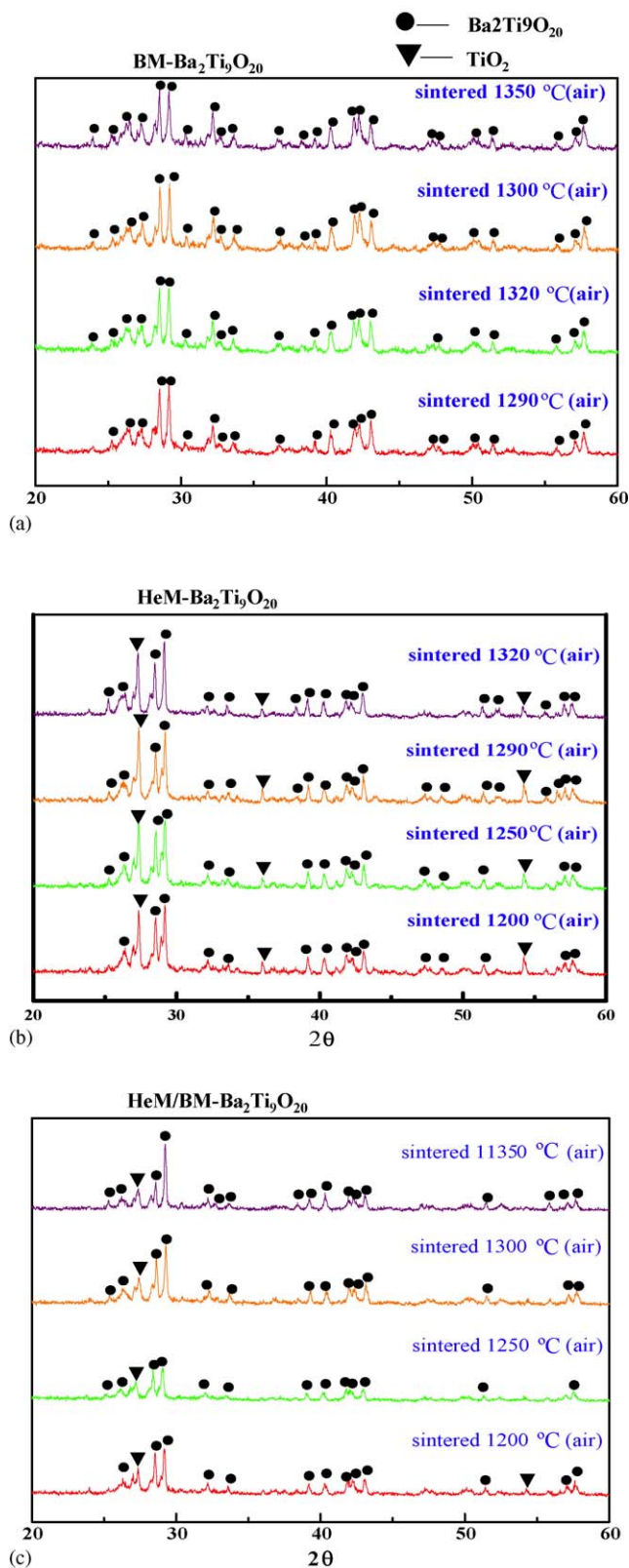


Fig. 1. The variation of X-ray diffraction patterns for  $\text{Ba}_2\text{Ti}_9\text{O}_{20}$  materials with sintering temperature. The samples were prepared from the  $\text{Ba}_2\text{Ti}_9\text{O}_{20}$  powders pulverized by (a) conventional ball-milling (BM) process, (b) high-energy-milling (HeM) process and (c) combined HeM/BM process.

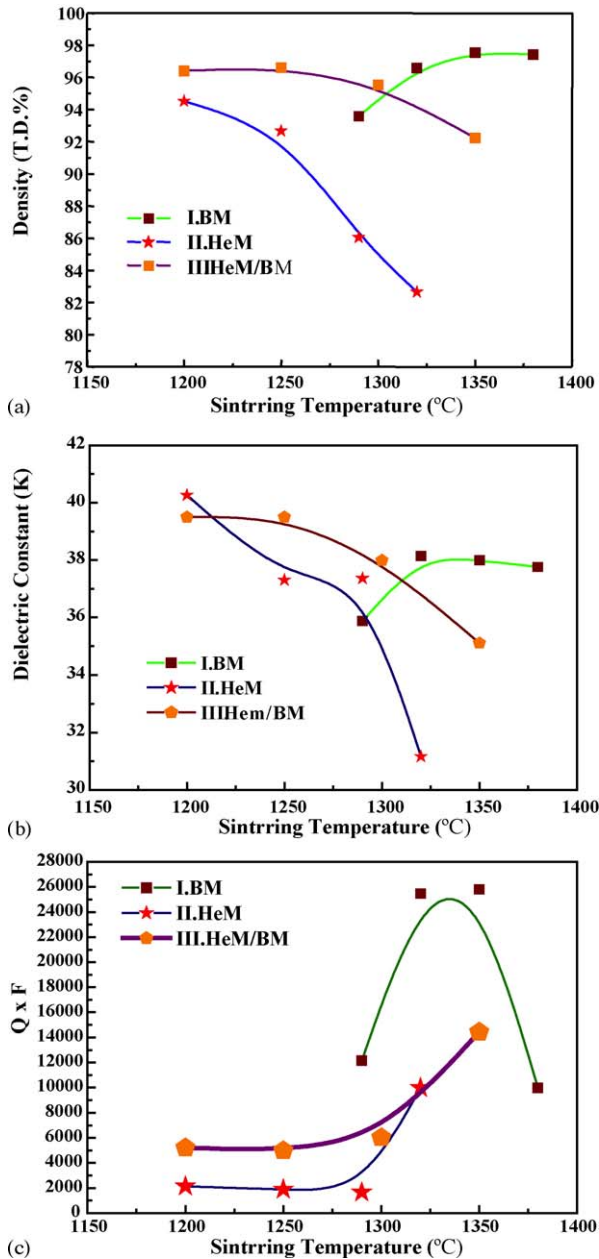


Fig. 2. The variation of (a) sintered density, (b) microwave dielectric constant ( $K$ ) and (c) microwave quality factor ( $Q \times f$ ) for  $\text{Ba}_2\text{Ti}_9\text{O}_{20}$  materials with sintering temperature. The samples were prepared from the  $\text{Ba}_2\text{Ti}_9\text{O}_{20}$  powders pulverized by (I) conventional ball-milling (BM) process, (II) high-energy-milling (HeM) process or (III) combined HeM/BM process.

cantly different from that of the BM-processed ones. The BM-processed samples contain bar-shaped grains with the size about  $4 \mu\text{m}$  in width and  $10 \mu\text{m}$  in length (Fig. 3(a)). The granular size distribution is quite uniform. In contrast, Fig. 3(b) indicates that the HeM-processed materials ( $1200^\circ\text{C}/4 \text{ h}$ ) contain rod-shaped grains with much higher aspect ratio and much smaller size. The grains are about  $1 \mu\text{m}$  in width and  $8 \mu\text{m}$  in length. Fig. 3(c) illustrates that sintering the HeM-processed samples at higher temperature ( $1320^\circ\text{C}/4 \text{ h}$ ) not only increases the aspect ratio of the grains, but also induces the presence of large grains of equiaxed geometry. EDAX analyses on these large grains (marked

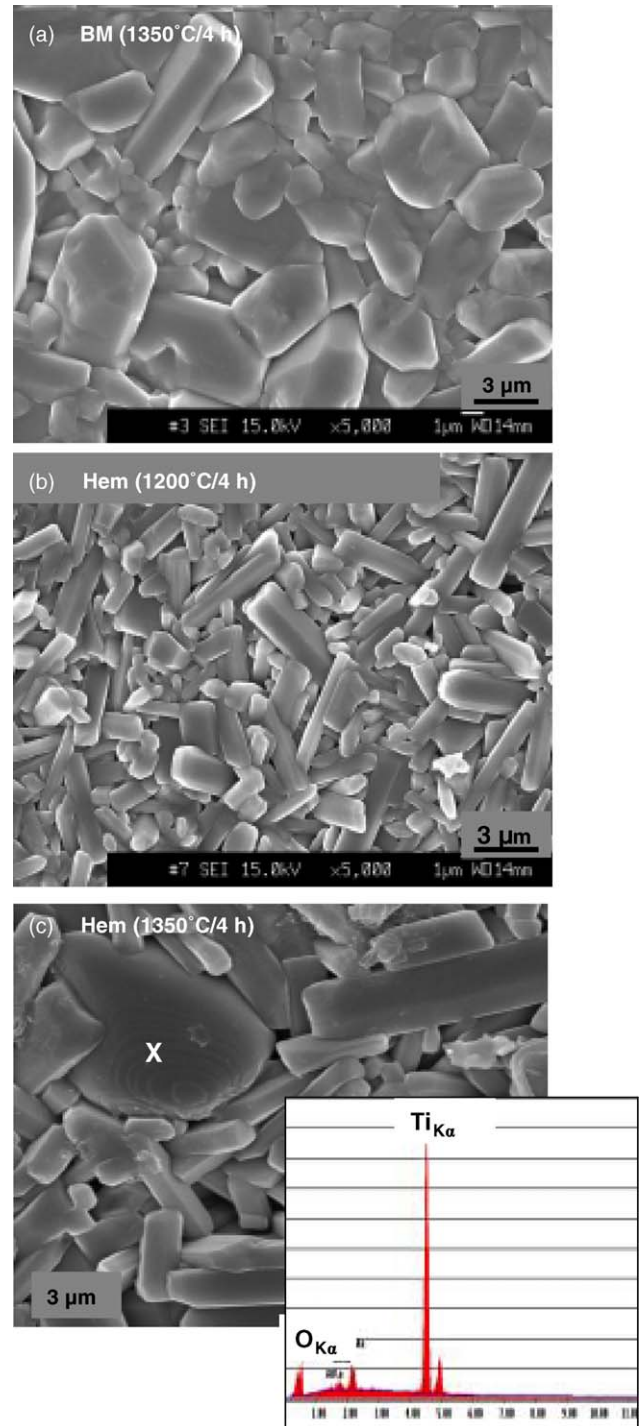


Fig. 3. SEM microstructure of  $\text{Ba}_2\text{Ti}_9\text{O}_{20}$  materials, which were prepared from (a) the conventional ball-milling (BM)-processed powders and sintered at  $1350^\circ\text{C}/4 \text{ h}$ , (b) the high-energy-milling (HeM)-processed powders and sintered at  $1200^\circ\text{C}/4 \text{ h}$  and (c), the high-energy-milling (HeM)-processed powders (sintered at  $1320^\circ\text{C}/4 \text{ h}$ ) and the inset showing the corresponding EDAX analysis of the grain indicated by "X".

"X") revealed that they are Ti-rich phase, as shown in the inset of Fig. 3(c). From these observations, SEM in Fig. 3(c) and XRD in Fig. 1(b), we can assign the secondary phase as  $\text{TiO}_2$ . The proportion of the  $\text{TiO}_2$  secondary phase increases with the sintering temperature.

Apparently, the HeM-processed powders are so active that they grow preferentially along *c*-axis of the crystals. Thereafter, the rod-grains with high aspect ratio is easily developed. The presence of the high aspect ratio rod-grains will induce the bridging of the grains, which will hinder the densification of the materials. Such a phenomenon is even more pronounced for the samples sintered at higher temperature, leading to the decrease in sintered density for these materials with the sintering temperature. Lower sintered density, accompanied by the induction of the secondary phase, will profoundly degrade the quality factor for the materials. Such a phenomenon accounts for the significantly lower  $Q \times f$ -value for the HeM-processed materials, as compared with those for the BM-processed ones.

One of the possible cause resulting in inferior microstructure and dielectric characteristics for the HeM-processed materials is that the HeM-processed powders are so fine that may be seriously agglomerated, which tends to grow preferentially along the *c*-axis of the grains, forming grains with high aspect ratio. Therefore, to suppress the formation of agglomerates for the HeM-processed powders, a ball milling in alcohol was applied after the high energy milling process, which is designated as HeM/BM process. Fig. 2(a) (curve III) illustrates the marked improvement on the densification efficiency for the  $\text{Ba}_2\text{Ti}_9\text{O}_{20}$  materials due to the post-ball-milling after HeM process. The density of the HeM/BM-processed samples already reached 96.2% T.D., when sintered at (1200 °C/4 h). The sintered density for the samples decreases moderately with sintering temperature. It should be noted that the HeM/BM-processed (1200 °C/4 h sintered) materials possess the same high density as the conventional BM-processed (1350 °C/4 h sintered) ones. Such a result implies that the modified HeM/BM process has markedly improved the sinterability for the  $\text{Ba}_2\text{Ti}_9\text{O}_{20}$  materials such that the samples can be sintered to a high density under lower sintering temperature.

XRD patterns in Fig. 1(c) show that the presence of  $\text{TiO}_2$  secondary phase is markedly suppressed for the samples prepared by HeM/BM process and were sintered below 1250 °C/4 h. Secondary phase starts to appear again when the sintering temperature increases over 1300 °C/4 h. SEM micrographs in Fig. 4(a) reveal that the grains are still of rod-shaped geometry, but the aspect ratio is pronouncedly reduced. The grains are about 0.8  $\mu\text{m}$  in width and 3  $\mu\text{m}$  in length and are uniformly distributed for the 1250 °C/4 h-sintered samples. Fig. 2(b) (curve III) indicates that the microwave dielectric constant ( $K$ ) of the HeM/BM materials is markedly larger than that of the HeM materials, which is apparently owing to the increase in sintered density. The microwave quality factor ( $Q \times f$ ) of the samples is also improved due to the ball-milling process (cf. Fig. 2(c), curves II and III). However, the dielectric constant of the HeM/BM materials also decreases with the sintering temperature (Fig. 2(b)). To understand this phenomenon, the evolution of microstructure due to the increase in sintering temperature was examined. Fig. 4(b) reveals that increasing the sintering temperature leads to marked increase in grain size, and will even induce the presence of secondary phases. These phenomena can account for the decreases in the sintered density and the degradation of the microwave dielectric properties due to the increase in sintering temperature.

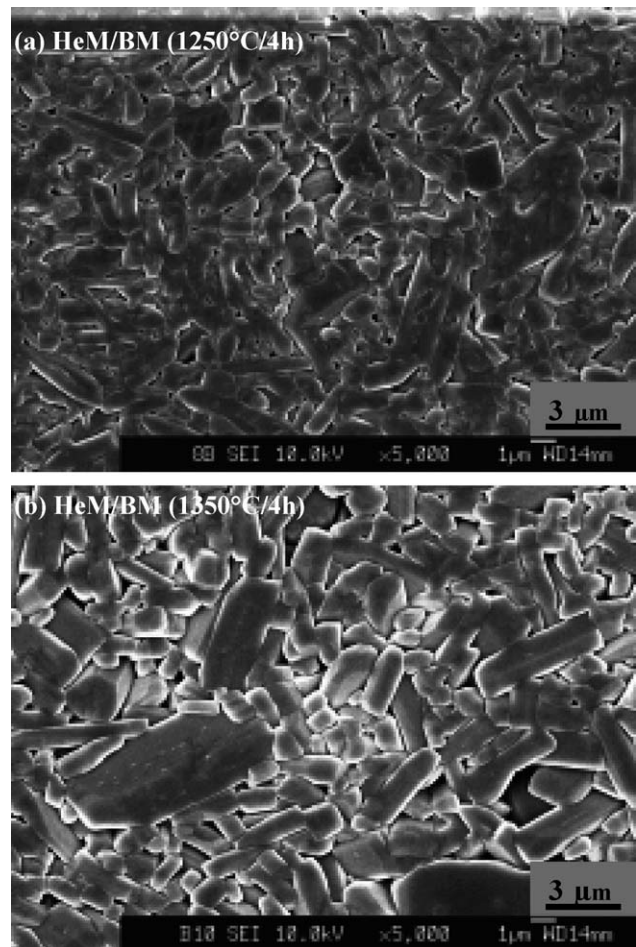


Fig. 4. SEM microstructure of  $\text{Ba}_2\text{Ti}_9\text{O}_{20}$  materials, which were prepared from the powders prepared by two-step process, including high-energy-milling (HeM) and ball-milling (BM) processes and sintered at (a) 1250 °C/4 h and (b) 1350 °C/4 h.

Although the HeM/BM processed (1250 °C/4 h-sintered) and BM-processed (1350 °C/4 h-sintered) samples have the same high density and are of Hollandite-like structure without the secondary phase, the microwave dielectric quality factor ( $Q \times f$ -value) of the HeM/BM-processed materials is significantly inferior to the BM-processed ones (cf. Fig. 2(c)). The factor resulting in inferior  $Q \times f$ -value for the former can be attributed to the significant difference in the granular structure for the two materials. Fig. 3(a) shows that the grains of the BM-processed samples are large-rods (4  $\mu\text{m} \times 10 \mu\text{m}$ ) with faceted surface, whereas Fig. 4(a) indicates that the grains of the HeM/BM-processed samples are small-rods (0.8  $\mu\text{m} \times 3 \mu\text{m}$ ) with round surface. Both the smaller grain size and the round geometry imply that the granular structure for the materials in the HeM/BM-processed samples are not completely developed.

To further investigate how the granular structure of  $\text{Ba}_2\text{Ti}_9\text{O}_{20}$  materials affects the microwave dielectric properties for the materials, lattice vibration modes of these two samples were examined by Raman spectroscopy. Fig. 5 indicates that the Raman spectra for the two samples are very complicated due to the complex in crystal structure (Hollandite-like). Unambiguously assigning each vibrational modes requires detailed

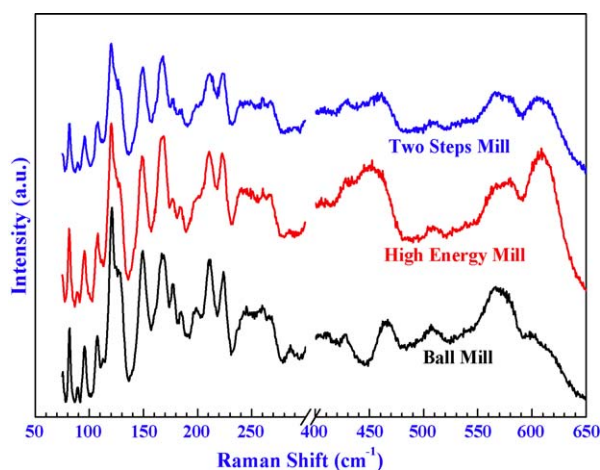


Fig. 5. Raman spectra of  $\text{Ba}_2\text{Ti}_9\text{O}_{20}$  materials, which were prepared from the conventional ball-milling (BM)-processed powders and sintered at  $1350^\circ\text{C}/4\text{ h}$ , the high-energy-milling (HeM)-processed or high-energy-milling and ball-milling two-step milling (HeM/BM)-processed powders and sintered at  $1250^\circ\text{C}/4\text{ h}$ .

analyses using first-principle calculation. However, simple comparison reveals that the resonance peaks of the Raman spectrum for BM-processed samples (spectrum I) are much sharper and contain more fine structure, as compared with those for the HeM/BM-processed samples (spectrum III). The sharper resonance peak indicates that the vibration of the lattices is more coherent, which is usually correlated with higher quality factor for the materials.<sup>15</sup> The vibrational characteristics of the lattices are intimately related with the uniformity of the bond strength between the ions in the materials. Smaller grain size for the HeM/BM-processed materials (cf. Fig. 4(a)) implies that there are larger proportions of ions located in the grain boundary region, which have fewer near-neighbor than the ions in the interior of the grains. Moreover, the rounded geometry for the HeM/BM-processed materials (cf. Fig. 4(a)) indicates that the surface atoms are not bonded very well with those in the interior of the grains, which further leads to the incoherency in the lattice vibration modes. That the coherency in lattice vibration modes is degraded, resulting in broadened Raman resonance peaks is frequently observed in the nanostructured materials. From the SEM microstructural examination, in conjunction with the Raman spectroscopic studies on the lattice vibrational characteristics, we can assume that the factor resulting in lower  $Q \times f$ -value for the HeM/BM-processed materials is the incompletely development in the granular structure for the materials.

#### 4. Conclusion

The influence of the processing technique on the characteristics of the  $\text{Ba}_2\text{Ti}_9\text{O}_{20}$  powders and the related microwave dielectric properties for the sintered  $\text{Ba}_2\text{Ti}_9\text{O}_{20}$  materials was investigated. Pure Holland-like structure was obtained when the

mixture of the nano-powders were directly calcined at  $1100^\circ\text{C}$ . The combined high-energy-milling and ball-milling (HeM/BM) process results in pronounced improvement for the sinterability of the  $\text{Ba}_2\text{Ti}_9\text{O}_{20}$  powders such that the samples attain a density higher than 96.2% T.D. by sintering the materials at  $1200^\circ\text{C}/4\text{ h}$ . However, the HeM/BM-processed samples show pronouncedly inferior microwave quality factor ( $Q \times f$ -value) to the BM-processed ones. Raman spectroscopic and SEM microstructure analyses imply that the prime factor resulting in lower  $Q \times f$ -value for HeM/BM-processed samples is the incomplete development of the granular structure.

#### Acknowledgement

The authors gratefully thank the financial support of the National Science Council, ROC for this research through the project no. NSC 93-2112-M032-010.

#### References

1. Jonker, G. H. and Kwestroo, W., Ternary system  $\text{BaO-TiO}_2\text{-SnO}$  and  $\text{BaO-TiO}_2\text{-ZrO}_2$ . *J. Am. Ceram. Soc.*, 1958, **41**(10), 390–394.
2. O'Bryan, H. M., Thomson Jr., J. and Plourde, J. K., A new  $\text{BaO-TiO}_2$  compound with temperature-stable high permittivity and low microwave loss. *J. Am. Ceram. Soc.*, 1974, **57**(10), 450–453.
3. O'Bryan, H. M. and Thomson Jr., J., Phase equilibrium in the  $\text{TiO}_2$ -rich region of the system  $\text{BaO-TiO}_2$ . *J. Am. Ceram. Soc.*, 1974, **57**(12), 22–526.
4. Fallon, G. D. and Gatehouse, B. M., The crystal structure of  $\text{Ba}_2\text{Ti}_9\text{O}_{20}$ : A Hollandite related compound. *J. Solid State Chem.*, 1983, **49**, 59–64.
5. O'Bryan, H. M., Grodkiewicz, W. H. and Bernstein, J. L., Preparation and unit-cell parameters of single crystals of  $\text{Ba}_2\text{Ti}_9\text{O}_{20}$ . *J. Am. Ceram. Soc.*, 1979, **63**(5–6), 309–310.
6. Grzanic, G. and Bursill, L. A., The Hollandite-related structure of  $\text{Ba}_2\text{Ti}_9\text{O}_{20}$ . *J. Solid State Chem.*, 1983, **47**, 151–163.
7. Tillmanns, E. et al., Crystal structure of the microwave dielectric resonator  $\text{Ba}_2\text{Ti}_9\text{O}_{20}$ . *J. Am. Ceram. Soc.*, 1983, **66**, 268–270.
8. Wu, J.-M. and Wang, H.-W., Factor affecting the formation of  $\text{Ba}_2\text{Ti}_9\text{O}_{20}$ . *J. Am. Ceram. Soc.*, 1988, **71**(10), 869.
9. Kim, D. J. and Kroeger, D. M., Optimization of critical current density of bulk YBCO superconductor prepared by coprecipitation in oxalic acid. *J. Mater. Sci.*, 1993, **28**, 4744.
10. Watanabe, A. and Haneda, H. H., Preparation of lead magnesium niobate by a coprecipitation method. *J. Mater. Sci.*, 1992, **27**, 1245.
11. Potar, H. S., Deshpande, S. B. and Date, S. K., Chemical coprecipitation of mixed (Ba+Ti) oxalates precursor leading to  $\text{BaTiO}_3$  powders. *Mater. Chem. Phys.*, 1999, **58**, 121.
12. Kim, S. et al., Preparation of barium titanate by homogeneous precipitation. *J. Mater. Sci.*, 1996, **31**, 3643.
13. Fang, T.-T. and Lin, H.-B., Thermal analysis of precursors of barium titanate prepared by coprecipitation. *J. Am. Ceram. Soc.*, 1990, **73**(11), 3363.
14. Chu, L.-W., Hsiue, G.-H. and Lin, I.-N. Characteristic of  $\text{Ba}_2\text{Ti}_9\text{O}_{20}$  microwave dielectric materials prepared by modified co-precipitation method. Private communication.
15. Chia, C. T., Chen, Y. C., Cheng, H. F. and Lin, I. N., Correlation of microwave dielectric properties and normal vibration modes of  $x\text{Ba}(\text{Mg}_{1/3}\text{Ta}_{2/3})\text{O}_3-(1-x)\text{Ba}(\text{Mg}_{1/3}\text{Nb}_{2/3})\text{O}_3$  ceramics: I. Raman spectroscopy. *J. Appl. Phys.*, 2003, **94**(5), 3360–3364.